CrystEngComm

ROYAL SOCIETY OF CHEMISTRY

COMMUNICATION

View Article Online
View Journal | View Issue

Check for updates

Cite this: *CrystEngComm*, 2025, **27**, 3887

Received 31st March 2025,
Accepted 13th May 2025

DOI: 10.1039/d5ce00357a

rsc.li/crystengcomm

Published on 16 May 2025. Downloaded by New Copenhagen University on 6/10/2025 2:28:08 PM.

A hydrogen-bonded organic framework with ultramicroporous channels based on proline and DL-2-phenoxypropionic acid†

Timothy Steenhaut, [a] Xiao Li,[ab] Fuli Zhou,[a] Koen Robeyns, [a] Tom Leyssens, *[a] Yaroslav Filinchuk*[a] and Oleksii Shemchuk[a]

The cocrystallization of two small, common organic molecules, namely DL-2-phenoxypropionic acid and DL-proline, resulted in the formation of a hydrogen-bonded organic framework with a large unit cell. The obtained solid displays a structure possessing unidimensional ultramicroporous channels, whose functionality was shown by dynamic water vapor sorption and reversible xenon sorption assessed by *in situ* X-ray powder diffraction.

The field of crystalline porous materials is one of the most booming topics in chemistry and materials science, as these show great promise in a large variety of applications ranging from catalysis to gas sorption and separation.[1–3] Zeolites, metal–organic frameworks (MOFs) and covalent organic frameworks (COFs) are the most representative examples, as they share a common feature, namely the interconnection of their building blocks by strong covalent or coordinative bonds.[4,5] It is only more recently that attention has been drawn towards hydrogen-bonded organic frameworks (HOFs), which rely on the assembly of organic building blocks through hydrogen-bonding interactions, leading to networks with potential porosity.[6] Although weaker in energy, the inherent features of hydrogen bonds (flexibility, moderate directionality, and reversibility) offer distinct properties and advantages to HOFs, notably related to their solution processability, simplicity of purification and potential of healing by simple recrystallization.[7] For these reasons, applications of HOFs are far-reaching, spanning across the fields of catalysis, energy, biomedical products, as well as the storage and separation of fine chemicals.[7]

Nonetheless, the development of stable HOFs with permanent porosity is not a straightforward task, as small molecules tend to pack closely in the solid-state,[8] and is typically the fruit of a joint effort based on molecular building block design and simulation tools. Identifying molecular crystals that have open channels or lattice voids and remain stable during the removal of guests, *e.g.* solvent molecules, by design is an almost impossible task, although recent studies have shown some progress in this direction.[9,10] However, such materials can be found serendipitously. Here, we present such a case, where a HOF made up only of DL-proline (PRO) and DL-2-phenoxypropionic acid (PPA) (Fig. 1A and B), two cheap common commercially available organic molecules, was discovered during mechanochemical cocrystal screening.

The particular PPA·PRO cocrystal presented here was encountered while searching for conglomerate forming systems between the two racemic compounds, according to a novel resolution tool that we recently introduced and discussed elsewhere.[11] However, conglomerate formation was not observed for PPA·PRO. Surprisingly, X-ray diffraction results showed that the combination of compounds presented herein show a rather remarkable outcome: regardless of the synthesis approach, whether it was through neat grinding or slurry mediated transformation, both molecules cocrystallized as PPA·PRO in a trigonal crystal

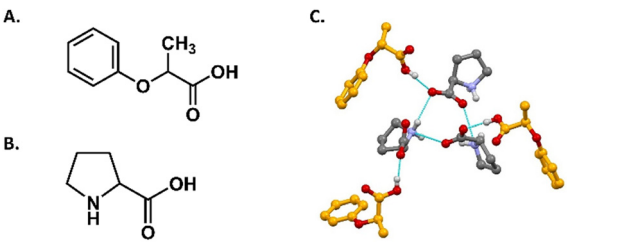

Fig. 1 Structures of (A) DL-2-phenoxypropionic acid (PPA) and (B) DL-proline (PRO), along with the (C) hydrogen bonding interactions (light blue) in the asymmetric unit of PPA·PRO. Hydrogen atoms linked to carbon are omitted for clarity (colour code: C from PPA = yellow; C from PRO = grey; O = red; N = purple; H = white).

[a] *Institute of Condensed Matter and Nanosciences, Place Louis Pasteur, 1 bte L4.01.03, BE-1348 Louvain-La-Neuve, Belgium. E-mail: tom.leyssens@uclouvain.be, yaroslav.filinchuk@uclouvain.be*

[b] *Hefei General Machinery Research Institute, Hefei, 230031, China*

† Electronic supplementary information (ESI) available: CCDC 2387025 and 2393897. For ESI and crystallographic data in CIF or other electronic format see DOI: https://doi.org/10.1039/d5ce00357a

Published on 16 May 2025. Downloaded by New Copenhagen University on 6/10/2025 2:28:08 PM.

system, space group $R\bar{3}$. Three pairs of molecules are present in the asymmetric unit (Fig. 1C), making in total 54 pairs of molecules per unit cell. While the *c*-axis measures only 5.6989(2) Å, the *a*- and *b*-axes are extremely long, reaching 62.932(2) Å. In this structure, prolines are in their zwitterionic form, and each of them forms a hydrogen bond with the carboxylate group of DL-2-phenoxypropionic acid. In addition, the carboxylate also forms two more hydrogen bonds with the protonated amines of two other proline molecules (Fig. 1C). Most interestingly, the overall structure of the obtained compound possesses small unidimensional ultramicroporous (*i.e.* <7 Å)[12] channels, large enough to accommodate small guest molecules (Fig. 2). Mercury software identifies the maximum pore diameter as 5.4 Å. Noticeably, even though other combinations were investigated (*e.g.* D-2-phenoxypropionic acid with L-proline), these never led to the formation of a HOF.

Prior to evaluating guest sorption, the thermal response of the HOF was investigated using thermogravimetric analysis (TGA), differential scanning calorimetry (DSC) and *in situ* synchrotron powder X-ray diffraction (see Fig. S1–S5†). TGA reveals negligible weight loss up to 130 °C, indicating that the organic moieties do not decompose below this temperature. Below 110 °C, the diffraction data indicate changes in relative peak intensities with temperature, likely ascribed to the release of adsorbed moisture. This corresponds to a weight loss of about 1.2% according to TGA. Above 100 °C, the intensities of Bragg peaks slowly fade away, disappearing above 130 °C. This is in accordance with DSC analysis results, revealing that melting occurs in this temperature range.

The interaction of PPA·PRO with water was further studied by dynamic vapour sorption (DVS) analysis. The most striking feature in the obtained isotherm is the presence of inflection points in the adsorption branch, coupled with hysteresis during desorption (Fig. 3). This behaviour indicates filling of the porous channels with water. Notably, a relative humidity

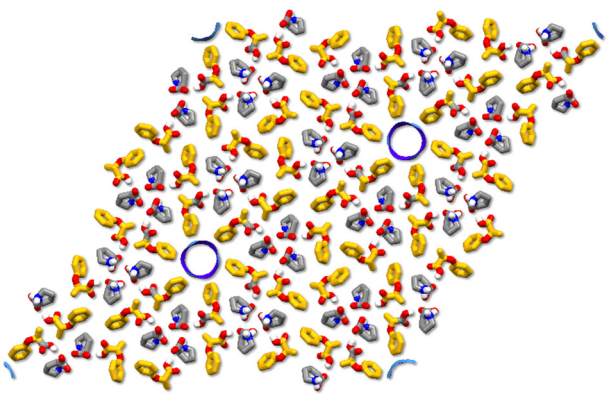

Fig. 2 Crystal packing of PPA·PRO, viewed along the *c*-axis. The boundaries of voids with a probe radius for Xe (radius = 198 pm, calculated using Mercury software) are displayed as blue circles. H(C) hydrogen atoms are omitted for clarity. Colour code: C from PPA = yellow; C from PRO = grey; O = red; N = deep blue; H = white.

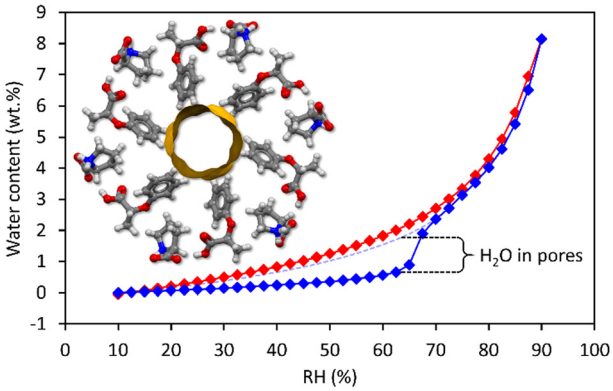

Fig. 3 Water sorption isotherm determined by dynamic vapour sorption, with adsorption in blue and desorption in red (the dotted blue line is a guide to the eye to evidence the amplitude of the hysteresis related to channel filling). The inset represents the boundary of voids with a probe radius for H_2O, represented in yellow (radius = 120 pm, calculated through Mercury software for crystal data analysis).

(RH) of around 65% is required before pore filling occurs, likely due to the hydrophobic nature of the aromatic rings that make up the pore walls. The total quantity of water adsorbed in the channels can be deduced by the amplitude of the hysteresis, which is close to the theoretical limit of 1.15 wt% H_2O, corresponding to the full occupancy of the pores (see the ESI† for details). An increase in the slope of water uptake is observed after the channels are completely filled. This suggests that once the voids are fully occupied by water, the material becomes more hydrophilic compared to its empty-pore counterpart. Furthermore, if stored at an RH below 60%, the material remains stable, with negligible water uptake.

The accessibility of the pores to guests was further assessed using N_2 and CO_2 sorption measurements. The nitrogen sorption isotherm at 77 K (Fig. S6†) exhibits a type-II behaviour, characteristic of non-porous solids according to the IUPAC classification. This indicates that the pores of PPA·PRO are not accessible to N_2 at this temperature.[12] From this isotherm, the (external) surface area was estimated through the Brunauer–Emmett–Teller (BET) equation to be 9.3 $m^2\ g^{-1}$. The Barrett–Joyner–Halenda (BJH) pore-size distribution, calculated from the N_2 sorption isotherm (Fig. S6B†), further suggests that most of the adsorption occurs on the external surface and in intergrain spaces. Additionally, the CO_2 isotherm at 0 °C shows only weak adsorption, with a linear trend. The dense crystallographic structure and the separation between the small porous channels likely contribute to the difficulty in distinguishing adsorption contributions from the external surface *versus* internal pores through conventional sorption measurements.

Therefore, the accessibility of the porous channels was unequivocally confirmed by the sorption of xenon as guest molecules at room temperature. With a kinetic diameter of 396 pm, this gas is expected to fit within the framework's channels (as verified using Mercury software, see Fig. 2).[13] The incorporation of gas molecules into the pores was

 This journal is © The Royal Society of Chemistry 2025

Published on 16 May 2025. Downloaded by New Copenhagen University on 6/10/2025 2:28:08 PM.

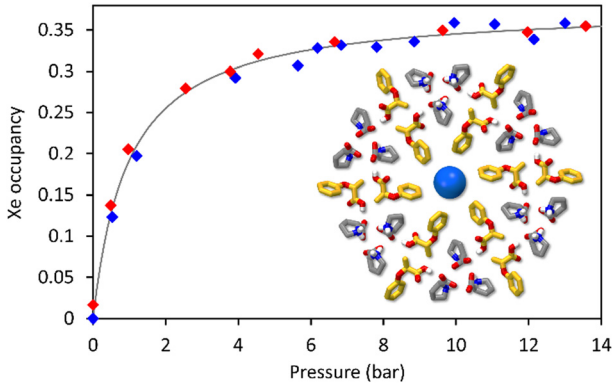

Fig. 4 Xenon sorption isotherm as determined from *in situ* XRPD. Experimental points are displayed in blue and red for adsorption and desorption, respectively, and the fit to the Langmuir equation is displayed as a grey curve. The inset represents xenon atoms in the porous channel viewed along the *c*-axis.

evaluated by means of *in situ* X-ray powder diffraction (XRPD) at different pressures, taking advantage of the significant difference in the electron density between xenon and the light atoms of the structure (for details, see the ESI†). Exposing the sample to Xe gas resulted in substantial changes in relative peak intensities of the XRPD pattern, indicating successful incorporation of the gas molecules into the framework channels. Rietveld refinement against the diffraction data allowed for the determination of guest positions and occupancies, which were plotted as a function of the applied pressure (see Fig. 4 and S7–S10†). Xe atoms occupy the special 6*c* Wyckoff site, which can be filled at most by 50%, given the presence of short mutually excluding Xe···Xe contacts along the channel. The obtained occupancies allowed for a good fit to the Langmuir equation, revealing a fully reversible type-I isotherm with a saturation occupancy of 0.38 Xe per adsorption site (Fig. 4), which is close to the limiting occupancy of 0.5. At the full limiting capacity, the unit cell would contain three Xe atoms, as compared to the 54 PPA·PRO units (2.6 wt%).

Upon closer examination of the H-bonded network in the title co-crystal, it becomes evident that, unlike most hydrogen-bonded organic frameworks, it does not exhibit extensive 2D or 3D H-bonded connectivity. Instead, it represents a rare example of a HOF with a 1D hydrogen-bonded network. These 1D HOFs arise when hydrogen bonding is restricted to linear or chain-like arrangements without significant cross-linking in higher dimensions, often forming chain or tubular structures. Consequently, the porous structure in this system is likely stabilized, at least in part, by non-covalent interactions such as π–π stacking and van der Waals forces. While most HOFs are designed for enhanced stability through extensive 2D or 3D hydrogen bonding, which reinforces structural robustness,[6] 1D hydrogen-bonded frameworks can also achieve stability through additional interactions, including π-stacking and interactions between hydrophobic groups. Similar 1D H-bonded architectures have been reported in the literature, further supporting the feasibility of such frameworks, but none of them were found to be porous.[14,15]

In summary, our study unveils a remarkable instance where a hydrogen-bonded organic framework (HOF) with an exceptionally large unit cell unexpectedly emerged from mechanochemical cocrystal screening involving proline and DL-2-phenoxypropionic acid. The structure of the resulting HOF exhibits unidimensional ultramicroporous channels capable of accommodating small guest molecules, as demonstrated through the incorporation of water and xenon gas, assessed through DVS and *in situ* XRPD, respectively. Owing to its small channels, this material shows promise for guest separation, especially considering the simplicity of its synthesis from two affordable and readily available molecules.

Data availability

The data supporting this article have been included as part of the ESI.†

Conflicts of interest

There are no conflicts to declare.

Acknowledgements

This work was supported by FNRS (PdR T.262.20 and T.0149.19, CdR J.0073.20 and J.0168.22). The authors acknowledge Dr. Dmitry Chernyshov for help with synchrotron XRPD measurements and Jean-François Statsyns for nitrogen sorption measurements. We acknowledge the FPS Economy of Belgium for funding through the Fonds de Transition Energétique (H2Be project). X. Li acknowledges the China Scholarship Council (CSC201706370133) and financial support of the Hefei General Machinery Research Institute Doctoral Science and Technology Funding (2023010788). The European Synchrotron Radiation Facility (ESRF) is acknowledged for beamtime allocation through proposal CH-6536 (metadata DOI: **https://doi.org/10.15151/ESRF-DC-2170175674**).

References

1 M. Eddaoudi, D. B. Moler, H. Li, B. Chen, T. M. Reineke, M. O'Keeffe and O. M. Yaghi, *Acc. Chem. Res.*, 2001, **34**, 319–330.
2 G. Ferey, *Chem. Soc. Rev.*, 2008, **37**, 191–214.
3 H. Furukawa, K. E. Cordova, M. O'Keeffe and O. M. Yaghi, *Science*, 2013, **341**, 1230444.
4 A. G. Slater and A. I. Cooper, *Science*, 2015, **348**, aaa8075.
5 J. Jiang, Y. Zhao and O. M. Yaghi, *J. Am. Chem. Soc.*, 2016, **138**, 3255–3265.
6 P. Li, M. R. Ryder and J. F. Stoddart, *Acc. Mater. Res.*, 2020, **1**, 77–87.
7 R. B. Lin, Y. He, P. Li, H. Wang, W. Zhou and B. Chen, *Chem. Soc. Rev.*, 2019, **48**, 1362–1389.

8 T. Hasell and A. I. Cooper, *Nat. Rev. Mater.*, 2016, **1**, 16053.
9 I. Hisaki, X. Chen, K. Takahashi and T. Nakamura, *Angew. Chem., Int. Ed.*, 2019, **58**, 11160.
10 X. Song, Y. Wang, C. Wang, D. Wang, G. Zhuang, K. O. Kirlikovali, P. Li and O. K. Farha, *J. Am. Chem. Soc.*, 2022, **144**, 10663.
11 F. Zhou, O. Shemchuk, M. D. Charpentier, C. Matheys, L. Collard, J. H. Ter Horst and T. Leyssens, *Angew. Chem., Int. Ed.*, 2021, **60**, 20264–20268.
12 M. Thommes, K. Kaneko, A. V. Neimark, J. P. Olivier, F. Rodriguez-Reinoso, J. Rouquerol and K. S. W. Sing, *Pure Appl. Chem.*, 2015, **87**, 1051–1069.
13 D. W. Breck, *Zeolite molecular sieves: structure, chemistry, and use*, Wiley, 1973.
14 B. Li, W. Qiu, G. P. A. Yap, Y. L. Dory and J. P. Claverie, *Adv. Funct. Mater.*, 2023, **34**, 2311964.
15 R.-B. Lin and B. Chen, *Chem*, 2022, **8**, 2114–2135.

Published on 16 May 2025. Downloaded by New Copenhagen University on 6/10/2025 2:28:08 PM.

This journal is © The Royal Society of Chemistry 2025